

Inverse identification processes of elastoplastic constitutive models using advanced optimisation strategies

B. Coelho¹, A. Andrade-Campos^{1,*}, J.M.P. Martins^{1,2}, T. Silva¹ and S. Thuillier²

¹Dep. of Mechanical Engineering, TEMA, University of Aveiro, Aveiro, Portugal.

²Univ. Bretagne Sud, UMR CNRS 6027, IRDL, F-56100 Lorient, France.

* Corresponding author (gilac@ua.pt)

Keywords: Calibration of constitutive models, Full-field measurements, Finite Element Model Updating, Virtual Fields Method, Optimisation efficiency, Metal plasticity.

Abstract

The success of simulation tools in reproducing the mechanical behaviour of materials, particularly for metals, depends on the quality of the models and their inherent material parameters. However, the commonly used parameter identification strategies are still expensive and non-robust. The robustness and efficiency of these strategies are closely related with the single-stage optimisation methods adopted.

The aim of this work is to implement and analyse optimisation strategies such as sequential, parallel and hybrid approaches in a parameter identification problem using full-field methods, particularly the Virtual Fields Method (VFM) and the Finite Element Model Updating (FEMU). The definition of the objective functions of both VFM and FEMU methods is also discussed in the framework of optimisation.

1. Introduction

Nowadays, there are a few solid numerical methodologies for extracting the material parameters from full-field strain measurements using digital image correlation (DIC) techniques. External methods, such as the FEMU, search for the parameter set that minimises the gap between the experimental and numerical observations. In these methods, a total separation between the experimental and the numerical data occurs. Equilibrium methods, such as the VFM, search for the parameter set that balances the internal and external work according to the principle of virtual work, where the internal work is calculated using the constitutive model applied to the experimental strain field [1-4]. Both methodologies use optimisation techniques to identify the parameters and, therefore, can undergo problems of initial solution's dependence, non-uniqueness of solution, local and premature convergence, physical constraints violation, *etc.*

In this work, the performance of gradient least-squares (GLS) and metaheuristic (MH) optimisation algorithms is compared. GLS algorithms are deterministic and search for local optimal solutions guided by the information of the derivatives. However, nonlinear optimisation problems may have several solutions that are locally optimal. MH algorithms, with their probabilistic nature, have the ability to obtain global optimal solutions, avoiding getting trapped in a local optimum. MH can be search-based (such as Simulated Annealing or Tabu Search), which focus on modifying and improving a single candidate solution, or population-based (such as Genetic Algorithms, Differential Evolution, *etc.*), which focus on improving multiple candidate solutions, often using population characteristics to guide the search.

Studies combining distinct implemented algorithms and parameter identification methods are performed in this work. Three case-studies are tested for checking the robustness of the strategies.

2. Problem Formulation

In this work, for the definition of the FEMU objective function, a combination of force (F) and in-plane strain components (ε_{xx} , ε_{yy} , ε_{xy}) is adopted. It can be described as:

$$f_{\text{FEMU}}(\mathbf{x}) = \frac{1}{n_s} \sum_{i=1}^{n_s} \left\{ \frac{1}{n_p} \sum_{j=1}^{n_p} \left[\sum_{k=xx,yy,xy} \left(\frac{\varepsilon_{i,j,k}^{\text{num}}(\mathbf{x}) - \varepsilon_{i,j,k}^{\text{exp}}}{\varepsilon_{i,j,k}^{\text{exp}}} \right)^2 \right] + \left(\frac{F_i^{\text{num}}(\mathbf{x}) - F_i^{\text{exp}}}{F_i^{\text{exp}}} \right)^2 \right\}, \quad (1)$$

where \mathbf{x} is the vector of decision variables (material parameters to be determined), n_s is the number of time-steps and n_p the number of in-plane measurement points.

The VFM objective function to be minimised is given by:

$$f_{\text{VFM}}(\mathbf{x}) = \frac{1}{n_s} \sum_{i=1}^{n_s} \left[\int_{\partial V} \mathbf{T} \cdot \mathbf{U}^* dS - \int_V \mathbf{P}(\mathbf{x}, \boldsymbol{\varepsilon}^{\text{exp}}) : \text{Grad } \mathbf{U}^* dV \right]^2, \quad (2)$$

where \mathbf{T} corresponds to the surface forces acting on the boundary ∂V of the specimen, V is the reference volume of the specimen, \mathbf{U}^* is the virtual displacement field, and $\mathbf{P}(\mathbf{x}, \boldsymbol{\varepsilon}^{\text{exp}})$ is the first Piola-Kirchhoff stress tensor.

4. Implementation, Results and Discussion

Results for the case-study represented in Fig. 1 are presented. The material model assumes: (i) isotropic elastic behaviour described by the generalised Hooke's Law; (ii) isotropic plastic behaviour described by the von Mises yield criterion and Swift's Law:

$$\sigma = K(\varepsilon_0 + \varepsilon_p)^n \quad \text{with} \quad \varepsilon_0 = \left(\frac{\sigma_0}{K} \right)^{1/n}, \quad (3)$$

where σ is the flow stress and ε_p is the equivalent plastic strain. K , the hardening coefficient, n , the hardening exponent, and σ_0 , the initial yield stress, form the set \mathbf{x} of material parameters to be identified. The numerical data generated by the finite element (FE) model is used as virtual experimental data, thus the reference parameters are known *a priori* ($\mathbf{x}_{\text{ref}} = [\sigma_0 = 160, n = 0.26, K = 565]$). The reference simulation was run with automatic increment control using ABAQUS/Standard, which required 30 increments/time-steps to complete the simulation. The implemented GLS optimisation algorithm is the Levenberg-Marquardt (LM) [5] using finite-differences Jacobian, and the MH algorithm is the Differential Evolution (DE) [6].

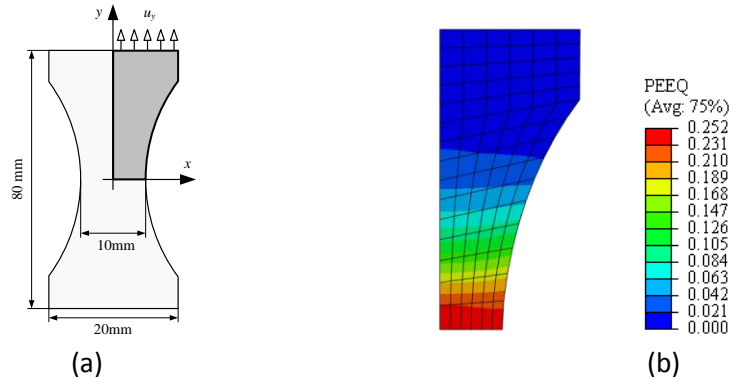


Figure 1. (a) Specimen geometry and (b) FE model showing the equivalent plastic strain distribution after a 3 mm displacement.

Tab. 1 lists the results for a 3-stage sequential strategy (GLS₁-MH-GLS₂) considering 2 starting sets (grey shading). The optimal solution obtained in each stage is used as the initial solution of the following stage. GLS₁ switches to MH after converging. MH uses the maximum number of evaluations as stopping criteria (4000 for VFM and 1000 for FEMU). Fig. 2 presents the evolution of the VFM objective function using the different starting sets. The results for the single MH are included for comparison purposes.

Table 1. VFM and FEMU results with the sequential strategy GLS₁-MH-GLS₂ considering two initial solutions (inf/sup). The initial and optimal values are provided. The optimal parameters' errors are calculated in relation to the reference set (\mathbf{x}_{ref}).

	GLS _{1,inf}				MH _{best}				GLS ₂			
	σ_0	n	K	f_{VFM}	σ_0	n	K	f_{VFM}	σ_0	n	K	f_{VFM}
Initial	100.4	0.080	165.0	4.5E+10	160.7	0.265	564.2	2.3E+05	160.1	0.261	560.1	2.1E+05
Optimal	160.7	0.265	564.2	2.3E+05	160.1	0.261	560.1	2.1E+05	160.7	0.265	564.2	2.3E+05
Err (%)	0.46	2.08	0.13	-	0.08	0.57	0.87	-	0.46	2.08	0.13	-
	GLS _{1,sup}				MH _{best}				GLS ₂			
	σ_0	n	K	f_{VFM}	σ_0	n	K	f_{VFM}	σ_0	n	K	f_{VFM}
Initial	234.7	0.350	965.0	3.2E+10	160.7	0.265	564.2	2.3E+05	160.1	0.261	560.1	2.1E+05
Optimal	160.7	0.265	564.2	2.3E+05	160.1	0.261	560.1	2.1E+05	160.7	0.265	564.2	2.3E+05
Err (%)	0.46	2.08	0.13	-	0.08	0.57	0.87	-	0.46	2.08	0.13	-
	GLS _{1,inf}				MH _{best}				GLS ₂			
	σ_0	n	K	f_{FEMU}	σ_0	n	K	f_{FEMU}	σ_0	n	K	f_{FEMU}
Initial	100.4	0.080	165.0	2.9E+00	85.6	0.092	169.2	2.3E+00	161.0	0.263	567.8	7.8E-04
Optimal	85.6	0.092	169.2	2.3E+00	161.0	0.263	567.8	7.8E-04	160.6	0.262	569.4	1.2E-04
Err (%)	46.50	64.78	70.04	-	0.64	1.02	0.50	-	0.37	0.87	0.78	-
	GLS _{1,sup}				MH _{best}				GLS ₂			
	σ_0	n	K	f_{FEMU}	σ_0	n	K	f_{FEMU}	σ_0	n	K	f_{FEMU}
Initial	234.7	0.350	965.0	3.2E-01	186.5	0.446	830.7	1.8E-01	163.0	0.265	577.6	1.2E-03
Optimal	186.5	0.446	830.7	1.8E-01	163.0	0.265	577.6	1.2E-03	162.2	0.266	578.4	9.0E-04
Err (%)	16.58	71.42	47.02	-	1.87	1.98	2.24	-	1.38	2.26	2.37	-

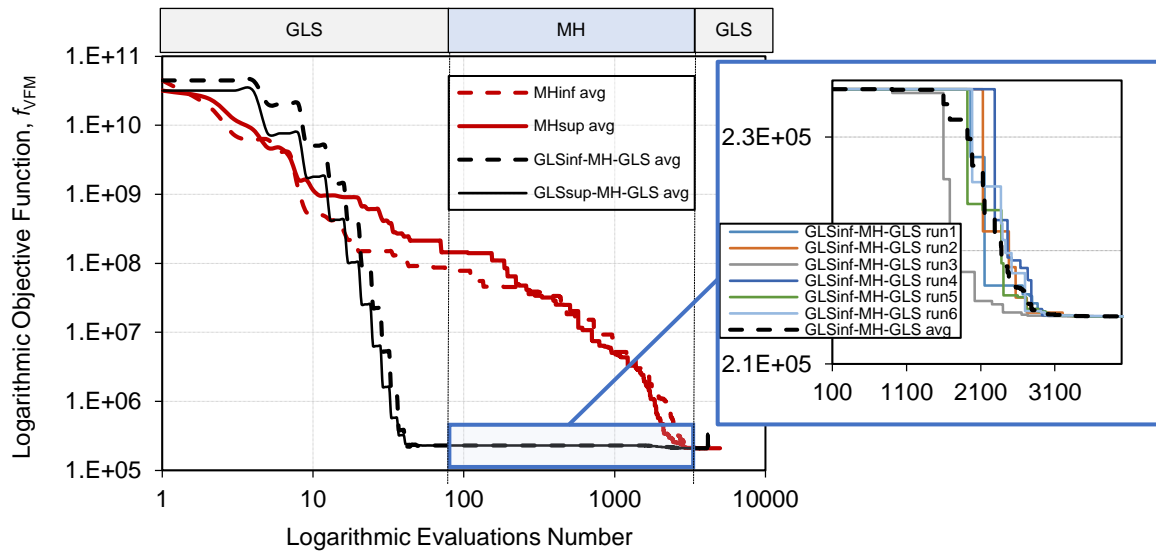


Figure 2. VFM objective function evolution with a sequential strategy considering two starting sets. A zoom-in (MH stage) shows the 6 runs that generated one of the curves.

With the VFM methodology, the GLS algorithm converges fast for a solution (less than 100 evaluations) with errors lower than 2%. However, although the MH required many evaluations to improve the solution, it found a solution with errors lower than 1% and with a large probability of being the global minimum. GLS revealed a non-dependence on the initial set since, in both stages, the algorithm converged always to the same solution. This observation reveals that the gradient-based evaluation performed by GLS differs from the direct evaluation of the objective function performed by MH. However, further investigations and an additional tuning of the GLS algorithm are required.

For the case of the FEMU method, a dependence of the GLS optimisation algorithm on the initial set is evident. In the first optimisation stage, GLS₁ was not capable of reaching admissible errors for the identified parameters. However, in the third stage, GLS₂ revealed to be capable of refining the search in the region of the global minimum previously found by the MH optimisation algorithm. GLS₂ provided an optimal solution with parameters' errors lower than 1% in the strategy starting with the inferior set ($\sigma_0 = 100.4$, $n = 0.08$ and $K = 165$) and up to 2% in the strategy starting with the superior set ($\sigma_0 = 234.7$, $n = 0.35$ and $K = 965$). As demonstrated in this case-study, since the MH algorithms do not depend on the initial solution, they reveal to be useful in providing an initial solution to GLS that is in the global optimum region.

5. Conclusions

When performing parameter identification, the choice of an optimisation algorithm is not straightforward. In this work, it is showed that metaheuristic algorithms can find better solutions, however with the cost of more evaluations. For a fast solution and errors up to 2%, the gradient-based least square algorithms are robust enough when using the VFM. The FEMU methodology revealed to be initial solution's dependent and to require a MH optimisation algorithm to find the global solution. Nevertheless, an optimisation strategy with sequential or parallel algorithms guarantees the global solution.

6. Acknowledgments

The authors acknowledge the financial support of FCT under the projects PTDC/EME-APL/29713/2017 (CENTRO-01-0145-FEDER-029713), PTDC/EMS-TEC/6400/2014 (POCI-01-0145-FEDER-016876), PTDC/EME-EME/31243/2017 (POCI-01-0145-FEDER-031243) and PTDC/EME-EME/30592/2017 (POCI-01-0145-FEDER-030592) by UE/FEDER through the programs CENTRO 2020 and COMPETE 2020, and UID/EMS/00481/2013-FCT under CENTRO-01-0145-FEDER-022083.

7. References

- [1] Cooreman S, Lecompte D, Sol H, Vantomme J, Debruyne D (2008) Identification of Mechanical Material Behavior Through Inverse Modeling and DIC. *Experimental Mechanics* 48: 421–433.
- [2] Haddadi H., Belhabib S. (2012) Improving the characterization of a hardening law using digital image correlation over an enhanced heterogeneous tensile test. *Int. J. Mech. Sci.* 62(1): 47-56.
- [3] Martins JMP, Andrade-Campos A, Thuillier S (2018) Comparison of inverse identification strategies for constitutive mechanical models using full-field measurements. *Int. J. Mech. Sci.* 145: 330-345.
- [4] Kim J-H, Serpantié A, Barlat F, Pierron F, Lee M-G (2013) Characterization of the post-necking strain hardening behavior using the virtual fields method. *Int. J. Solids Struct.* 50(24): 3829–3842.
- [5] Nocedal, J, Wright, S. (2006) *Numerical Optimization*, Springer-Verlag New York.
- [6] Storn, R.; Price, K. (1997). Differential evolution - a simple and efficient heuristic for global optimization over continuous spaces. *Journal of Global Optimization* 11: 341–359.